EFFICIENCY OF TEXTURE MEASUREMENT FROM TWO OPTICAL SENSORS FOR IMPROVED BIOMASS ESTIMATION

J. E. Nichol, M. L. R. Sarker

Department of Land Surveying and Geo-Informatics, The Hong Kong Polytechnic University
Kowloon, Hong Kong - lsjanet@polyu.edu.hk

KEY WORDS: AVNIR-2, SPOT-5, texture measurement, biomass estimation, image processing

ABSTRACT:

No technique has so far been developed to quantify biomass carbon sources and sinks over large areas. Among the remote sensing techniques tested, the use of multisensors, and spatial as well as spectral characteristics of data have demonstrated strong potential for biomass estimation. However, the use of multisensor data accompanied by spatial data processing has not been fully investigated because of the unavailability of appropriate data sets and the complexity of image processing techniques for combining multisensor data with the analysis of spatial characteristics. This research investigates the texture parameters of two high (10m) resolution optical sensors AVNIR-2 and SPOT-5 in different processing combinations for biomass estimation. Multiple regression models are developed between image parameters extracted from the different stages of image processing and the biomass of 50 field plots, which was estimated using a newly developed "Allometric Model" for the study region.

The results demonstrate a clear improvement in biomass estimation using the texture parameters of a single sensor (r^2=0.854 and RMSE=38.54) compared to the highest accuracy obtained from simple spectral reflectance (r^2=0.494) and simple spectral band ratios (r^2=0.59). This accuracy was further improved, to obtain a very promising accuracy using texture parameters of both sensors together (r^2=0.897 and RMSE=32.38), the texture parameters from the PCA of both sensors (r^2=0.851 and RMSE=38.80) and the texture parameters from the averaging of both sensors (r^2=0.911 and RMSE=30.10). Improved accuracy was also observed using the simple ratio of texture parameters of AVNIR-2 (r^2=0.899 and RMSE=32.04) and SPOT-5 (r^2=0.916) and finally a surprisingly high accuracy (r^2=0.939 and RMSE=24.77) was achieved using the ratios of the texture parameter of both sensors together.

1. INTRODUCTION

Remote sensing is the most promising technique to estimate biomass at local, regional and global scales, thereby helping to reduce the uncertainties associated with the role of forests in key environmental issues (Brown et al, 1989; Rosenqvist et al 2003). A number of studies has been carried out using different types of sensors including optical (Mukkönen and Heiskännen, 2005; Fuchs et al 2009; Foody et al, 2003; Dong et al, 2003) SAR (Santos et al, 2003; Kuplich et al, 2005), and Lidar sensors (Zhao et al 2009) for biomass/forest parameter estimation. Apart from the use of a single sensor, combining information from multiple sensors has yielded promising results for the estimation of forest parameters/biomass (Rosenqvist et al, 2003; Hyde et al, 2006; Boyd and Danson, 2005.

Although vegetation indices, have been successfully used in temperate forests Zheng et al, 2004; Rahman et al, 2005), they have shown less potential in tropical and subtropical regions where biomass levels are high, the forest canopy is closed with multiple layering, and great diversity of species is present (Foody et al, 2001, 2003; Boyd et al, 1996; Lu, 2005). On the other hand, the spatial characteristics of images have such as texture have been found particularly useful in fine spatial resolution imagery (Franklin et al, 2001; Boyd and Danson, 2005), and capable of identifying different aspects of forest stand structure, including age, density and leaf area index (Champion et al, 2008; Wulder et al, 1996). Indeed, texture has shown potential for biomass estimation with both optical (Franklin et al, 2001; Lu, 2005; Fuchs et al, 2009) and SAR data (Santos et al, 2003; Lu, 2005; Kuplich et al, 2005) Moreover, although most previous biomass estimation projects used Landsat TM data with a 30m spatial resolution (Lu, 2006), texture is expected to be more effective with finer spatial resolution imagery since finer structural details can be distinguished (Kuplich et al, 2005; Boyd and Danson, 2005; Franklin et al, 2001). This research investigates texture processing for biomass estimation using data from two high resolution optical sensors ANVIR-2 and SPOT-5 along with raw spectral processing and some simple band ratios. The overall objective of the study is to explore the potential of texture processing combined with multisensor capability for the improvement of biomass estimation using data from two high resolution optical sensors.

The study area for this research is the Hong Kong Special Administrative Region (Fig. 1) which lies on the southeast coast of China, just south of the Tropic of Cancer. Approximately 40% of Hong Kong is designated as Country Parks which are reserved for forest succession. The native sub-tropical evergreen broad leaf forest has been replaced by a complex patchwork of regenerating secondary forest in various stages of development, and plantations. Forest grades into woodland, shrubland then grassland at higher elevations.

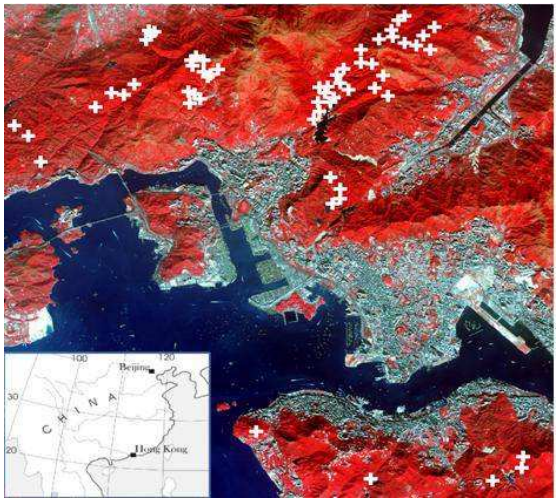

Figure 1. Study area and location of field sampling plots

2. METHODOLOGY

The methodology (Fig. 2) of this study comprises two parts namely allometric model development for field biomass estimation, and processing of AVNIR-2 and SPOT-5 images. Due to the lack of an allometric model for converting the trees measured in the field to actual biomass, it was necessary to harvest, dry and measure a representative sample of trees. Since tree species in Hong Kong are very diverse, the harvesting of a large sample was required. This was done by selecting the dominant tree species comprising a total of 75 trees in 4 DBH classes (less than 10, 10-15, 15-20 and 20 & above cm) and standard procedures were followed for tree harvesting (Ketterings et al, 2001; Overman et al, 1994).

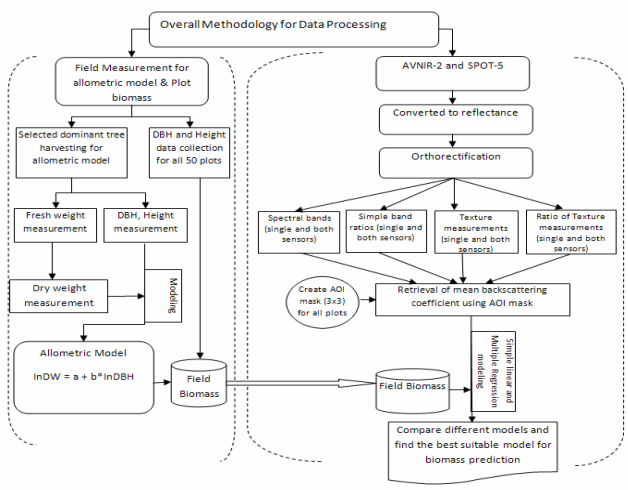

Figure 2. Overall methodology of this research

The harvested trees were separated into fractions including leaves, twigs, small branches, large branches and stem. After measuring the fresh weight, representative samples from every part of the tree were taken for dry weight measurement in an oven at 80°C temperature until a constant dry weight was obtained (Fig 3). The weight of every sample was estimated using the same electric weight balance at 0.002gm precision. The ratio of dry weight (DW) to fresh weight (FW) was calculated for every part of the samples using DW and FW of each part of the tree. Using the ratio, DW was calculated for every part, and finally the DW of each tree was calculated by summing the DW of all parts.

Figure 3. Preparing the samples for dry weight measurement

Regression models using DW as the dependent variable, and DBH and height as independent variables were tested, and the best fit model (Table 2) was found to be InDW = a+b*In DBH, with the adjusted coefficient of determination (adjusted r^2 0.932) and an RMSE of 13.50. This was deemed highly satisfactory in view of the great variety of tree species, and is similar to the accuracies of several other specialist forest inventories (Brown et al, 1989; 1997; Overman et al, 1994).

To build a relationship between image parameters and field biomass, 50 circular plots with a 15m radius covering a variety of tree stand types were selected using purposive sampling. The DBH of trees was measured at 1.3 m above ground and the heights of small and large trees were measured by Telescopic-5 and DIST pro4 respectively. Using the measured parameter DBH, the biomass of each tree and biomass of all trees in a plot were estimated

3. IMAGE PROCESSING

The DN of the AVNIR-2 and SPOT data were converted to Spectral Radiance, and the images were orthorectified using the Satellite Orbital Math Model to obtain RMS error within 0.5 pixel. All individual spectral bands of AVNIR-2 and SPOT-5 as well as different combinations of band ratios and PCA were tested for biomass estimation. All individual spectral bands of AVNIR-2 and SPOT-5 as well as different combinations of band ratios and PCA were tested for biomass estimation. Additionally, nineteen different types of texture measurements (Table 1) from GLCM based (Haralick, 1973) and SADH based (Unser, 1986) were used to generate texture parameters from 4 spectral bands each of AVNIR-2 and SPOT data using 4 window sizes (3x3 to 9x9). All the generated parameters were tested by comparison with the field biomass using stepwise and multiple regression models of single and dual-sensor data.

Gray level co-occurrence matrix (GLCM) based texture

1. $Mean(ME) = \sum_{i,j=0}^{N-1} i\, P_{i,j}$

2. $Homogeneity(HO) = \sum_{i,j=0}^{N-1} i \frac{P_{ij}}{1+(i-j)^2}$

3. $Contrast(CO) = \sum_{i,j=0}^{N-1} i\, P_{i,j}\, (i-j)^2$

4. $Standard\ deviation(Std) = \sqrt{VA}$

   $where\ VA == \sum_{i,j=0}^{N-1} i\, P_{i,j}\, (i-ME)^2$

5. $Dissimilarity(DI) = \sum_{i,j=0}^{N-1} i\, P_{i,j}\, |i-j|$

6. $Entropy(EN) = \sum_{i,j=0}^{N-1} i\, P_{i,j}\, (-\ln P_{i,j})$

7. $Angular\ Second\ Moment\ (ASM) = \sum_{i,j=0}^{N-1} i\, P_{ij}^2$

8. $Inverse\ Difference\ (ID) = \sum_{i,j=0}^{N-1} i \frac{P_{ij}}{|i-j|^2}$

9. $GLDV\ Angular\ Second\ Moment\ (GASM) = \sum_{k=0}^{N-1} V_k^2$

10. $GLDV\ Entropy\ (GEN) = \sum_{k=0}^{N-1} V_k\, (-\ln V_k)$

P (i, j) is the normalized co-occurrence matrix such that SUM (i , j=0, N-1) (P (i, j)) = 1.
V(k) is the normalized grey level difference vectorV(k) = SUM (i, j=0, N-1 and |i-j | = k) P (i, j)

Sum & difference histogram (SADH) based texture parameter

1. $Mean\ (\mu) = \frac{\sum_{i,j} x_{ij}}{n}$

2. $Mean\ deviation\ (MD) = \frac{\sum_{i,j} |x_{ij} - \mu|}{n}$

3. $Mean\ Euclidean\ distance\ (MED) = \sqrt{\frac{\sum_{i,j} (x_{ij} - x_c)^2}{n-1}}$

4. $Variance\ (\sigma^2) = \frac{\sum_{i,j} (x_{ij} - \mu)^2}{n-1}$

5. $Normalized\ Coefficient\ of\ Variation(NCV) = \sqrt{\frac{\sigma^2}{\mu}}$

6. $Skewness\ (Sk) = \frac{\sum_{i,j} (x_{ij} - \mu)^3}{(n-1)\sigma^3}$

7. $Kurtosis\ (Ku) = \frac{\sum_{i,j} (x_{ij} - \mu)^4}{(n-1)\sigma^4}$

8. $Energy(E) = \sum_{i,j} X_{ij}^2$

9. $Entropy\ (H) = -\sum_{i,j} p_{ij} \ln(p_{ij}), \quad with\ p_{ij} = \frac{x_{ij}}{\sum_{i,j} x_{ij}}$

X_{ij} = pixel value of pixel (i, j) in kernel, n = the number of pixels that is summed, x_c = the kernel's center pixel value, p_{ij} = the normalized pixel value.

Table 1. Formulae of texture measurements used in this study

4. RESULTS AND ANALYSIS

The field biomass data from the 50 field plots ranged from 52t/ha to 530t/ha. In all modeling processes, the 50 field plots were used as the dependent variable and parameters (AVNIR-2 and/or SPOT-5) derived from different processing steps were used as independent variables.

The best estimates of biomass using simple spectral bands of AVNIR-2 and SPOT-5 as well as different combinations of band ratios and PCA produced only ca. 60% useable accuracy due to (i) the complexity of forest structure and terrain in the study areas, (ii) The very high field biomass in this study area (52t/ha to 530t/ha), and (iii) strong multicollinearity effects among the 8 bands and band ratios from the two sensors used.

A notable improvement was observed for both sensors using texture parameters (Table 2). For single band texture, the highest (ANVIR r^2= 0.742 and SPOT-5 r^2 = 0.769) and lowest (ANVIR r^2=0.309 and SPOT-5 r^2=0.326) accuracies were obtained from the texture parameters of NIR and Red bands respectively. The pattern of accuracy was similar to that obtained using raw spectral bands although the performance was much higher for texture measurement. Moreover, as with raw data, the second highest accuracies (ANVIR r^2=0.547 and SPOT-5 r^2=0.615) were also obtained from green and SWIR bands using AVNIR-2 and SPOT-5 data respectively. These patterns of improvement were consistent for both sensors and very much in agreement with the general behavior of interaction between different wavelengths and vegetation. Thus we found that texture measurement enhanced biomass estimation across all bands but greater improvement was observed from the bands where reflectance from vegetation is higher.

However, unlike raw spectral bands and simple ratios of raw spectral bands, texture parameters from all bands together (either all bands of AVNIR-2 or SPOT-5) were found to be very useful, and obtained accuracies of 0.786 (r^2 for AVNIR-2) (model 1 in Table 2) and 0.854 (r^2 for SPOT-5) (model 2 in Table 2) Apart from the improved accuracies the developed models (using all texture parameters of an individual sensor together) were significant and no multicollinearity effects were evident.

When texture parameters from both sensors were combined together in the model (model 3 in Table 2), as well as all texture parameters of PCA of both sensors together (model 4 in Table 2), and all texture parameters from averaging of both sensors together (model 5 in Table 2), very significant improvements were obtained although PCA was not found to be very effective. The highest (r^2=0.91) and the second highest (r^2=0.90) accuracies were obtained from the texture parameters from the averaging of both sensors, and texture parameters of both sensors in the model respectively. These differences were attributed to the fact that averaging is a type of data fusion, and

the synergy between the two sensors probably contributed complementary information in the model.

Model	R^2	RMS error
1. Texture parameters of AVNIR-2 all bands ME_AB4_5, Ku_AB2_9, CO_AB4_9, TEN_AB3_9, Sk_AB2_5, Ske_AB1_9	0.79	46.5
2. Texture parameters of SPOT-5 all bands Sk_SB3_9, ASM_SB1_9, HO_SB4_9, ID_SB3_5, ID_SB2_3, GASM_SB4_5	0.85	38.5
3. Texture parameters of both sensors combined ASM_SB1_9, ASM_AB4_9, HO_AB4_7, Sk_SB3_7, Var_SB3_9, GEN_SB4_7, MDM_AB3_5	0.90	32.4
4. Texture parameters from PCA both sensors ASM_BPC1_9, CO_BPC3_9, Sk_BPC1_7, Var_BPC2_9, Var_BPC1_9, Std_BPC1_5, MED_BPC3_3/4_3	0.85	38.8
5. Texture parameters from Average of both sensors Ku_A4+S4_7, ASM_A2+S1_9, Ku_A2+S1_5, Sk_A4+S3_7, Var_A4+S3_9, ASM_A4+S3_9, HO_A3+S2_3	0.91	30.1
6. Texture parameter ratio of AVNIR-2 GEN_AT1/4_9, ASM_AT2/3_7, GEN_AT2/3_7, DI_AT2/3_9, Std_AT2/4_5, TME_AT2/4_9, ME_AT3/4_9, Ku_ST2/3_5	0.90	32.0
7. Texture parameter ratio of SPOT-5 Sk_ST3/4_9, DI_ST2/4_7, Var_ST3/4_9, ASM_ST1/2_5, MDM_ST3/4_7, CO_ST2/4_9, GEN_ST3/4_9	0.92	29.1
8. Texture parameter ratio of both sensors DI_ST2/4_7, Sk_ST3/4_9, Var_ST3/4_9, ASM_ST1/2_5, MDM_ST3/4_7, CO_ST2/4_9,GEN_ST3/4_9, MDM_aT2/3_5 CO_AT2/3_7	0.94	24.8

Table 2. Results of biomass estimation. For models (ME, Ku, CO etc, see Table 1. AB4_5 means AVNIR Band 4 with kernel 5*5, and SB3_7 means SPOT Band 3 with 7*7 kernel.

Finally, the ratio of texture parameters was found to be more effective for biomass estimation compared to the highest accuracies obtained from all previous steps. The accuracies obtained using all ratios of texture parameters of AVNIR-2 (r^2=0.899) (model 6 in Table 2), SPOT-5 (r^2=0.916) (model 7 in Table 2) and the texture ratios of both sensors together (r^2=0.939) (model 8 in Table 2) were considerably higher than for the simple texture models. Similar to the texture models, no multicollinearity effects were evident.

This great improvement in biomass estimation observed in this study can be explained by the fact that we used three image processing techniques together as follows;

(i) texture processing which had already shown potential for biomass estimation in many previous studies using optical (Fuchs et al, 2009; Lu, 2005) and SAR data (Santos et al, 2003; Kuplich et al, 2005).

(ii) datasets from two different sensors were used in this processing. Although both datasets used are from optical sensors (AVNIR-2 and SPOT-5), there are differences in the wavebands, therefore it was anticipated that at least some complementary information could be obtained.

(iii) finally we tested the ratio of texture parameters. We know from previous research that ratios, whether simple or complex, and whether between different bands, different polarizations, or different frequencies, can improve biomass estimation by minimizing features which are similar in both bands such as topographic and forest structural effects.

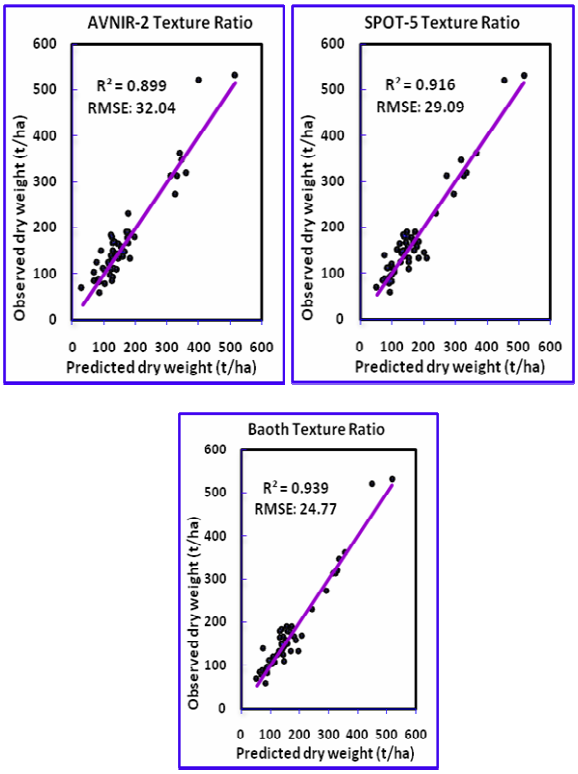

Figure 3. Relationship between field and model biomass

5. CONCLUSION

Data from two high resolution optical sensors were used in this research to establish a relationship between field biomass and remotely sensed observation parameters. The processing of data was conducted for each sensor individually and both sensors together. Spectral reflectance, texture parameters and ratio of texture parameters were evaluated for the improvement of biomass estimation. The results are promising, and except for the simple spectral reflectance, the accuracy (r^2) of biomass varied estimation was higher than 80%, though this varied between the two sensors due to different band availability. The accuracy of SPOT-5 sensor was somewhat higher in all processing steps compared to AVNIR-2 except for the simple spectral reflectance because of the availability of SPOT's SWIR band. However, better results were obtained using data from both sensors because of the complementary information.

In this research we obtained accuracy (r^2) ranging from 0.79 to 0.94 using different processing steps, and the highest accuracy (r^2=0.94) was obtained using the texture parameter ratio of both sensors. This accuracy is very promising, and this achievement

can be explained by our step wise processing which included the advantages of texture, ratio and complementary information from different sensors. In addition to the remote sensing data processing, the comprehensive and study area-specific nature of the field biomass data, and demonstrated accuracy of the allometric model (i.e. r^2 of 0.93) devised for this study from the destructive sampling of 75 trees was instrumental in obtaining this high accuracy. This research used numerous processing steps and data combinations, but in other field conditions a similar approach can be adopted to identify the most suitable steps for that particular situation.

ACKNOWLEDGMENTS

The authors would like to acknowledge the Hong Kong Agriculture, Fisheries and Conservation Department (AFCD) for help with tree harvesting in country parks, as well as the Japan Aerospace Exploration Agency (JAXA) for the ALOS images under ALOS agreement no. 376. This project was also sponsored by GRF grant no. PolyU5281/09E.

REFERENCES

Boyd, D. S. Foody, G. M. Curran, P. J. Lucas R. M., Honzak, M. 1996. An assessment of radiance in Landsat TM middle and thermal infrared wavebands for the detection of tropical forest regeneration, International Journal of Remote Sensing, 17, pp.249-261.

Boyd D. S., Danson, F. M. 2005. Satellite remote sensing of forest resources: Three decades of research development, Progress in Physical Geography, 29, pp.1-26.

Brown, S. A. Gillespie J. R., Lugo, A. E. 1989. Biomass estimation methods for tropical forests with applications to forest inventory data, Forest Science, 35, pp.881-902.

Brown., S. 1997. Estimating biomass and biomass change of tropical forests: A primer. FAO, USA.

Champion, I. Dubois-Fernandez, P. Guyon D., Cottrel, M. 2008. Radar image texture as a function of forest stand age, International Journal of Remote Sensing, 29, pp.1795-1800.

Dong, J. Kaufmann, R. K. Myneni, R. B. Tucker, C. J. Kauppi, P. E. Liski, J. Buermann, W. Alexeyev V., Hughes, M. K. 2003. Remote sensing estimates of boreal and temperate forest woody biomass: Carbon pools, sources, and sinks, Remote Sensing of Environment, 84, pp.393-410.

Foody, G. M. Cutler, M. E. McMorrow, J. Pelz, D. Tangki, H. Boyd D. S., Douglas, I. 2001. Mapping the biomass of Bornean tropical rain forest from remotely sensed data, Global Ecology and Biogeography, 10, pp.379-387.

Foody, G. M., Boyd D. S., Cutler, M E J, 2003. Predictive relations of tropical forest biomass from Landsat TM and transferability between regions, Remote Sensing of Environment, 85, pp.463-474.

Fuchs, H. Magdon, P. Kleinn C., Flessa, H. 2009. Estimating aboveground carbon in a catchment of the Siberian forest tundra: Combining satellite imagery and field inventory, Remote Sensing of Environment, 113, pp.518-531.

Haralick, R. M. Shanmugam K., Dinstein, I. 1973. Textural features for image classification, IEEE Transactions on Systems, Man and Cybernetics, smc 3, 610-621.

Hyde, P. Dubayah, R. Walker, W. Blair, J. B. Hofton M., Hunsaker, C. 2006. Mapping forest structure for wildlife habitat analysis using multi-sensor (LiDAR, SAR/InSAR, ETM+, Quickbird) synergy, Remote Sensing of Environment, 102, pp.63-73.

Kuplich, T. M. Curran P. J. and Atkinson, P. M. 2005. Relating SAR image texture to the biomass of regenerating tropical forests, International Journal of Remote Sensing, 26, pp.4829-4854.

Lu, D. 2005. Aboveground biomass estimation using Landsat TM data in the Brazilian Amazon, International Journal of Remote Sensing, 26, pp.2509-2525.

Lu, D. 2006. The potential and challenge of remote sensing-based biomass estimation, Int. J. Remote Sens., 27, 1297-1328,
Muukkönen P., Heiskänen, J. 2005. Estimating biomass for boreal forests using ASTER satellite data combined with standwise forest inventory data, Remote Sensing of Environment, 99, pp.434-447.

Overman, J. P. M., Witte H. J. L., Saldarriaga, J. G., 1994. Evaluation of regression models for above-ground biomass determination in Amazon rainforest, Journal of Tropical Ecology, 10, pp.207-218.

Rahman, M. M. Csaplovics E. and Koch, B. 2005. An efficient regression strategy for extracting forest biomass information from satellite sensor data, International Journal of Remote Sensing, 26, pp.1511-1519.

Santos, J. R. Freitas, C. C. Araujo, L. S. Dutra, L. V. Mura, J. C. Gama, F. F. Soler L. S., 2003. Airborne P-band SAR applied to the aboveground biomass studies in the Brazilian tropical rainforest, Remote Sensing of Environment, 87, pp.482-493.

Unser, M., 1986. 1986. Sum and difference histograms for texture classification. IEEE Transactions on Pattern Analaysis and Machine Intelligence, PAMI-8, pp.118-125.

Wulder, M. A., Franklin S. E., Lavigne, M. B. 1996. High spatial resolution optical image texture for improved estimation of forest stand leaf area index, Canadian Journal of Remote Sensing, 22, pp.441-449.

Zhao, K. Popescu S., Nelson, R. 2009. Lidar remote sensing of forest biomass: A scale-invariant estimation approach using airborne lasers, Remote Sensing of Environment, 113, pp.182-196.

Zheng, D. Rademacher, J. Chen, J. Crow, T. Bresee, M. Le Moine J., Ryu, S. -, 2004. Estimating aboveground biomass using Landsat 7 ETM+ data across a managed landscape in northern Wisconsin, USA, Remote Sensing of Environment, 93, pp.402-411,